Comparative Biochemistry and Physiology, Part A 155 (2010) 309–318

Contents lists available at ScienceDirect

Comparative Biochemistry and Physiology, Part A

journal homepage: www.elsevier.com/locate/cbpa

Na^+/K^+-ATPase and vacuolar-type H^+-ATPase in the gills of the aquatic air-breathing fish *Trichogaster microlepis* in response to salinity variation

Chun-Yen Huang [a], Pei-Lin Chao [a], Hui-Chen Lin [a,b,*]

[a] Department of Life Science, Tunghai University, Taichung 40704, Taiwan
[b] Center for Tropical Ecology and Biodiversity, Tunghai University, Taichung 40704, Taiwan

ARTICLE INFO

Article history:
Received 20 September 2009
Received in revised form 10 November 2009
Accepted 10 November 2009
Available online 18 November 2009

Keywords:
Na^+/K^+-ATPase
Vacuolar-type H^+-ATPase
Aquatic air-breathing fish
Osmoregulation
Trichogaster microlepis

ABSTRACT

The aquatic air-breathing fish, *Trichogaster microlepis*, can be found in fresh water and estuaries. We further evaluated the changes in two important osmoregulatory enzymes, Na^+/K^+-ATPase (NKA) and vacuolar-type H^+-ATPase (VHA), in the gills when fish were subjected to deionized water (DW), fresh water (FW), and salinated brackish water (salinity of 10 g/L). Fish were sampled only 4 days after experimental transfer. The mortality, plasma osmolality, and Na^+ concentration were higher in 10 g/L acclimated fish, while their muscle water content decreased with elevated external salinity. The highest NKA protein abundance was found in the fish gills in 10 g/L, and NKA activity was highest in the DW and 10 g/L acclimated fish. The VHA protein levels were highest in 10 g/L, and VHA activity was highest in the DW treatment. From immunohistochemical results, we found three different cell populations: (1) NKA-immunoreactive (NKA-IR) cells, (2) both NKA-IR and HA-IR cells, and (3) HA-IR cells. NKA-IR cells in the lamellar and interlamellar regions significantly increased in DW and 10 g/L treatments. Only HA-IR cells in the lamellar region were significantly increased in DW. In the interlamellar region, there was no difference in the number of HA-IR cells among the three treated. From these results, *T. microlepis* exhibited osmoregulatory ability in DW and 10 g/L treatments. The cell types involved in ionic regulation were also examined with immunofluorescence staining; three ionocyte types were found which were similar to the zebrafish model.

1. Introduction

Teleosts have highly efficient osmoregulatory mechanisms to maintain internal homeostasis. Fish gills, which are constantly exposed to external environments, are multifunctional organs important for various homeostatic activities such as gas exchange, ion regulation, and acid–base balance (Perry, 1997, 1998; Hirose et al., 2003; Evans et al., 2005). The four pairs of branchial arches consist of many filaments and lamellae that are covered with epithelial cells. Pavement cells, mitochondria-rich cells (MRCs, formerly chloride cells), mucous cells, and undifferentiated cells are known as the four major cell types in the gill epithelia (Perry, 1997; Evans, 1999). Pavement cells make up more than 90% of the gill surface (mostly in the lamellae) and are considered the site of gas exchange (Moron and Fernandes, 1996; Evans, 1999). Mitochondria-rich cells generally are distributed in the filaments and inter- and basal-lamellar regions and are believed to be the site of ion extrusion in seawater fish and ion uptake in fresh water fish (Perry, 1998; Evans, 1999; Evans et al., 2005; Hwang and Lee, 2007). The membrane-spanning enzyme Na^+/K^+-ATPase (NKA) in MRCs is important for intracellular homeostasis and provides a driving force for many transporting systems.

Air-breathing fishes are fish with the ability to exchange gases directly with the aerial environment, and they are further classified into amphibious and aquatic air-breathing modes (Graham, 1997). The accessory air-breathing organs include skin, lungs, respiratory gas bladders, labyrinth organ, digestive tracts, and structures derived from buccal, pharyngeal, and branchial cavities (Graham, 1997). Previous studies on the Anabantoidei mostly concerned vascular organization by examining cardiac and/or vascular casts (Burggren, 1979; Munshi et al., 1986; Olson et al., 1986, 1994, 1995; Olson, 2002). No evidence is available to determine whether morphological modifications are directly related to their functional differentiation. We had previously reported the morphological and functional differences between the anterior and posterior gill arches in the anabantoid fish, *Trichogaster leeri* (Huang et al., 2008). The anterior gills responsible for ion regulation increase NKA enzyme activity and the number of MRCs in deionized water (DW). Large-bore arterioarterial shunts and shorter lamellae in the fourth gill arch are specialized for the transport of oxygenated blood and are less responsive to environmental stress (Huang et al., 2008). However, other specific proteins involved in osmoregulatory functions remained unclear.

In fresh water, gills transport Na^+ and Cl^- actively from the environment. Two models have been proposed for Na^+ uptake in the

* Corresponding author. Department of Life Science, Tunghai University, Taichung 40704, Taiwan. Tel.: +886 4 23500461; fax: +886 4 23590296.
E-mail address: hclin@thu.edu.tw (H.-C. Lin).

1095-6433/$ – see front matter © 2009 Elsevier B.V. All rights reserved.
doi:10.1016/j.cbpa.2009.11.010

MRCs: the use of the electroneutral exchange of Na^+ and H^+ by the Na^+/H^+ exchanger (NHE) (Hirose et al., 2003; Evans et al., 2005; Hwang and Lee, 2007; Watanabe et al., 2008), and the involvement of the epithelial Na^+ channel (ENaC) together with active H^+ excretion by the vacuolar-type H^+-ATPase (VHA) (Hirose et al., 2003; Perry et al., 2003; Hwang and Lee, 2007). Further, the model for Cl^- uptake is supported by the presence of an apical $Na^+/K^+/2Cl^-$ cotransporter (NKCC) or Na^+/Cl^- cotransporter (NCC) that transfers ions from the environment into the cell and to body fluids through basolateral NKA and Cl^- channels (Hwang and Lee, 2007; Hiroi et al., 2008). Another mechanism was found in zebrafish larvae, Cl^- uptake depended on Cl^-/HCO_3^- exchangers under normal conditions (Bayaa et al., 2009). Hwang and Lee identified three subtypes of ionocytes, including: (1) NaR (NKA-rich) cells; (2) HR (VHA-rich and NKA-few) cells; and (3) NCC (thiazide-sensitive Na^+/Cl^- cotransporter-expressing) cells, by using immunocytochemistry and in situ hybridization in zebrafish embryo skins (Hwang and Lee, 2007; Hwang, 2009). Therefore, it is necessary to determine the distribution and functions of ion-transport proteins among various cells.

Na^+/K^+-ATPase and VHA are known to participate in ion regulation in fishes. Teleosts will up-regulate NKA activity in response to environmental changes (Morgan and Iwama, 1998; Kelly et al., 1999a,b; Imsland et al., 2003) and this is attributed to increased NKA α-subunit mRNA abundance (Scott et al., 2004), protein abundance (Lin et al., 2003), or both (Lin et al., 2004, 2006). In zebrafish, VHA plays a role in the uptake of Na^+ by using a specific morpholino to knock down VHA and impair Na^+ uptake activity (Horng et al., 2007). Moreover, experiments in killifish have demonstrated that VHA is involved in Na^+ uptake in low-NaCl fresh water (Katoh et al., 2003), but the location and role of absorbing chloride actively across the gills in freshwater is unclear now (Patrick and Wood, 1999).

This study aimed to determine whether gill NKA and VHA differ in their expression in an aquatic air-breathing fish, *Trichogaster microlepis* across a range of salinities. Individuals of the genus *Trichogaster* inhabit freshwater and estuarine environments and are distributed in Taiwan and southeastern Asia (http://fishbase.sinica.edu). We compared mortality, plasma osmolality and Na^+ concentration, muscle water content (MWC), environmental stress indicators (i.e., heat shock proteins, hsp70 and 90), gill NKA and VHA responses (including protein abundance and enzyme activity), and the amounts of the NKA-immunoreactive (NKA-IR) cells and VHA-immunoreactive (HA-IR) cells acclimated to salinities ranging in DW and 10 g/L treatments. In addition, we also examined the distribution of NHE, NKA, NKCC and VHA among osmoregulatory cells by the immunofluorescence staining.

2. Materials and methods

2.1. Animal and experimental tanks

T. microlepis (either sex, 4–6 cm in standard length) (Perciformes, Anabantoidei, Osphronemidae) has a natural habitat similar to that of *T. leeri* described in our previous study (Huang et al., 2008). We purchased the fish from a local fish shop and maintained them in plastic tanks ($45\times25\times30$ cm^3) with aerated, circulating local tap water filled to a height of 20 cm. One fifth of the water was replaced every 3 days. The fish were acclimated at 28 ± 1 °C under a 12 h:12 h light:dark cycle and fed with commercial fish food (NOVO Bits, JBL, Germany) once daily for at least a week before the experiment. The fish were not fed during the experiments. The oxygen levels (Orion model 810, UK) and pH (Jenco, pH vision 6071, HK) were monitored in the experimental tanks. The experiments and handling of the animals complied with the current laws of Taiwan.

For the experimental tanks, we used plastic tanks ($26\times15\times15$ cm^3). For all treatments, the tanks were filled to a height of 14 cm unless otherwise stated. Aerated and filtered local tap water was used for freshwater treatment (FW, control treatment). Deionized water (DW treatment) was prepared using a water purification system (Milli-Q plus system, Millipore, USA). Salinated brackish water (10 g/L and 15 g/L treatments) was prepared by mixing deionized water and artificial salts (Coralife Scientific Grade Marine Salt, USA) and the salinity was monitored by a refractometer (ATAGO Model S; Mill-E, Japan). No bottom sand was provided. There were 8 fish for all treatments. Water chemistry is summarized in Table 1.

2.2. Osmolality analysis and ionic concentration

Fish were anesthetized with MS-222 [0.4 g, 3-aminobenzoic acid ethyl ester (Sigma, USA), diluted to 1 L with experimental water] and subsequently sacrificed. The blood was collected by directly puncturing the heart with a 29-gauge needle (29 ga × 1/2 in., U-100; TERUMO, Japan). Blood was immediately centrifuged (EBR12R, Hettich, Germany) at 20,160 *g* for 10 min at 4 °C, and plasma osmolality was determined with a vapor pressure osmometer (Wescor Model 5500; Wescor Inc., Logan, UT, USA) using 10 μL aliquots. Water osmolality was determined simultaneously. The Na^+ concentrations of the water and plasma were measured by an atomic absorption spectrophotometer (Z-5000; Hitachi, Japan).

2.3. Muscle water content

The muscles from the dorsal trunk of the fish from the DW, FW, 10 g/L, and 15 g/L groups were excised. Water and blood on the muscle were removed with tissue paper. MWC was determined by the percentage of weight loss after drying at 100 °C (Thermolyne 6000; Furnace, USA) for 3 days.

2.4. Protein extraction

The first gill was homogenized in 200 μL homogenizing medium. The homogenizing medium was prepared from a mixture of proteinase inhibitors and buffer solution in a volumetric ratio of 1:200. The proteinase inhibitors contained (in mM) antipain 3.31, leupeptin 2.16, and benzamidine 63.86 in aprotinin saline solution (5–10 trypsin inhibitor units per mL, Sigma-Aldrich, USA, Cat. No. A6279). The buffer solution contained (in mM) imidazole (imidazole-HCl buffer) 100, Na_2EDTA 5, sucrose 200, and sodium deoxycholate 0.1%. The pH was maintained at 7.6. To obtain the supernatants, the crude homogenate was centrifuged at 20,160 *g* for 5 min twice at 4 °C (Ultrasonic Processor, SONICS, USA). The fresh supernatants were immediately analyzed. Then, 2 μL of supernatant was further diluted to 200 μL with deionized water. An aliquot of 100 μL of this mixture was further diluted to 800 μL with deionized water (800-fold). This diluted supernatant was mixed well with 200 μL of protein assay solution (Bio-Rad). Total protein levels were determined by a spectrophotometer (U-2001; Hitachi, Japan) at a wavelength of 595 nm. Bovine serum albumin diluted with redeionized water by the same dilution factor was prepared as a control. All chemicals used in the experiment were obtained from Sigma (USA) and Merck (Germany), unless mentioned otherwise.

Table 1
Water chemistry and fish mortality in the experiments.

	DW	FW	10 g/L	15 g/L
pH	7.14 ± 0.08*	7.81 ± 0.10	7.67 ± 0.07	7.61 ± 0.12
Osmolality (mOsm/kg)	0.22 ± 0.18*	3.26 ± 1.02	290.64 ± 5.75*	427.30 ± 12.37*
Na^+ (mM)	0.05 ± 0.02*	1.24 ± 0.28	99.28 ± 9.18*	120.29 ± 32.05*
Mortality	4.26% (2/47)	4.17% (2/48)	12.77% (6/47)	100% (8/8)

Values are presented as mean ± SEM. ($N=10$). The asterisk indicates a significant difference compared to the control group ($p<0.05$, Dunnett's *t*-test). Mortality was calculated as the number of dead fish divided by the number of fish tested.

2.5. Antibodies

The antibodies were NKA α-subunits (NKA, 1:1000, α-5 monoclonal antibody; from chicken, DSHB, USA), $Na^+/K^+/2Cl^-$ cotransporter (NKCC, 1:1000, T4 monoclonal antibody which recognized NKCC1 and NKCC2; from human, DSHB, USA), heat shock protein 70 (hsp70, 1:5000, monoclonal antibody; from mouse, Sigma, USA), and β-actin (1:10,000, monoclonal antibody; from mouse, Chemicon, USA). Other antibodies used in the experiment included VHA (1:2500, based on the highly conserved and hydrophilic region in the α-subunit from pufferfish, polyclonal antibody; a gift from Dr. Tsung-Han Lee at the University of Chung-Hsing, Taiwan), Na^+/H^+ exchanger (NHE, 1:15,000, polyclonal antibody; from Japanese dace; a gift from Dr. Toyoji, Kaneko at the Tokyo University, Japan), and heat shock protein 90 (hsp90, 1:5000, polyclonal antibody; from mouse, Cell Signaling Technology, USA). The secondary antibodies included alkaline phosphate conjugated goat-anti-mouse IgG and anti-rabbit IgG (Jackson Immunoresearch Laboratories, West Grove, PA, USA) to detect the above primary antibody. All the antibodies were used in the following study.

2.6. Immunoblotting analysis of protein abundance

Ten micrograms of whole-gill homogenate were solubilized in a sample-loading buffer (20 mM Tris–HCl, pH 6.8, 8% sodium dodecyl sulfate (SDS), 20% β-mercaptoethanol, 40% glycerol, and 0.4% bromophenol blue). Proteins were denatured at different temperatures and were separated on 10% and 12% SDS-polyacrylamide gels. After electrophoresis, the protein was transferred from the gel to a polyvinylidene difluoride membrane (Amersham, NEN Life Science, Boston, MA, USA). The membranes were blocked in 5% non-fat milk in PBST (containing in mM: NaCl 136.9, KCl 2.68, $Na_2HPO_4 \cdot 2H_2O$ 6.39, KH_2PO_4 1.76, and 0.5% Tween 20, pH 7.4) for 1 h at room temperature (RT: 26 °C). Subsequently, membranes were washed in PBST and incubated with the monoclonal primary antibody (NKA, 1:1000) and polyclonal primary antibody (VHA, 1:2500) for 1 h at RT, respectively. Membranes were washed again in PBST three times for 15 min, and they were then conjugated with anti-mouse and anti-rabbit secondary antibodies (1:10,000) for 1 h at RT. After washing with PBST three times for 15 min, the proteins were detected using western blot chemiluminescence reagent plus system (NEN Life Science) to identify the concerned proteins. The signals were captured and photographed by an Intelligent Dark Box II with Fujifilm LAS-1000 digital camera and the relative protein abundance was estimated and analyzed by Image Gauge 4.0 (Fujifilm). The relative protein abundance was the target protein divided by β-actin (internal control) in each set.

2.7. NKA and VHA enzyme activity

Enzyme-specific activity was determined by differences between the inorganic phosphate liberated in the presence and absence of protein inhibitors. Ouabain and bafilomycin A_1 were used as inhibitors for NKA and VHA, respectively. The inorganic phosphate concentration was modified according to the method of Peterson (1978) using microplates. Stock reaction buffer containing (in mM) imidazole (imidazole-HCl buffer) 142.85, NaCl 178.5, $MgCl_2$ 10.71, and KCl 107.14 was prepared in advance. The pH was maintained at 7.6. Each sample was assayed in triplicate. For measuring NKA activity, the inhibitor-free solution (1600 μL) comprised 800 μL of reaction buffer, 200 μL of 10 mM sodium azide, 200 μL of 2.5 μM bafilomycin A_1, and 400 μL of redeionized water. The ouabain-inhibitor solution (1600 μL) comprised 800 μL of reaction buffer, 200 μL of 10 mM sodium azide (inhibits F-type ATPase), 200 μL of 2.5 μM bafilomycin A_1, 200 μL of 10 mM ouabain, and 200 μL of redeionized water. For measuring VHA activity, the inhibitor-free solution (1600 μL) comprised 800 μL of reaction buffer, 200 μL of 10 mM sodium orthovanadate (inhibits P-type ATPase), 200 μL of 10 mM sodium azide, 200 μL of 10 mM ouabain, 200 μL of DMSO, and 200 μL of redeionized water. The bafilomycin A_1-inhibitor solution (1600 μL) comprised 800 μL of reaction buffer, 200 μL of 10 mM sodium orthovanadate, 200 μL of 10 mM sodium azide, 200 μL of 10 mM ouabain, 200 μL of 2.5 μM bafilomycin A_1, and 200 μL of redeionized water. In each well, 2 μL of gill lysates were added to 40 μL of mixed inhibitor-free or enzyme-inhibitor solution. Then, 10 μL Na_2ATP 30 mM was added and incubated at 37 °C for 30 min. Using 100 μL of Bonting's color reagent ($FeSO_4$ 176 mM, H_2SO_4 560 mM, and ammonium molybdate tetrahydate 8.1 mM) the solution was shaken and incubated at 20 °C for 30 min in the dark. The inorganic phosphate concentration was recorded at 690 nm using the spectrophotometer (ELISA, Enzyme Linked ImmunoSorbent Assay; Thermo, USA). Enzyme-specific activity is expressed as $\mu mol\ Pi \cdot mg^{-1}\ protein \cdot h^{-1}$.

2.8. Immunohistochemical detection of NKA- and VHA-immunoreactive (NKA- and HA-IR) cells

First gill arches were excised and fixed in Bouin's solution for 48 h at 4 °C in the dark. These samples were rinsed with phosphate buffer solution (PBS) followed by ethanol–xylene series dehydration. The PBS was prepared using (in mM) NaCl 136.9, KCl 2.68, $Na_2HPO_4 \cdot 2H_2O$ 10.15, and KH_2PO_4 1.76 in redeionized water to make 1 L of solution with a pH of 7.4. After embedding in paraffin, tissue sections were prepared with a thickness of 4–5 μm (RM2025RT; Leica, Germany) and placed on slides precoated with poly-L-lysine solution. The samples were dewaxed and rehydrated before staining with hematoxylin and eosin. They were dehydrated again, mounted, and examined by a light microscope (E600; Nikon, Japan).

The rehydrated samples were next immersed in 3% H_2O_2 (in 100% methanol) for 10 min to remove any endogenous reaction followed by a 2-min wash with PBS three times. The NKA primary antibody (1:20,000) and VHA primary antibody (1:10,000) was applied for 1.5 h in the dark at RT. After washing for 2 min with PBS three times, the secondary antibody (HRP/Fab polymer conjugate, Zymed) and the color reagent (aminoethyl carbazole signal solution chromogen (AEC kit), Zymed) were applied for 30 and 15 min, respectively. Lastly, the samples were stained by hematoxylin (Zymed) for 1 min. The samples were mounted (GVA mounting solution, Zymed) and examined using a light microscope (E600; Nikon, Japan). Pictures were taken by a digital camera (D1; Nikon, Japan) and saved to a computer. Slides of the negative control without the application of the primary antibody were prepared simultaneously.

First, the consecutive sections were used to characterize which cells contained both NKA and VHA from the FW treatment. If cells of consecutive sections both had the NKA- and VHA-immunoreactive, these cells were defined the NKA and VHA co-localized. Second, eight fishes were randomly chosen for quantifying the numbers of the NKA-IR cells and HA-IR cells in the lamellae and interlamellar region in each experimental treatments. Only those NKA-IR cells and HA-IR cells in the lamellae that were 5 μm away from the base of the lamellae were included. The lengths of the lamellae and interlamellar regions were determined by image processing software (Image-Pro Plus 4.5; Media Cybernetics, Silver Spring, MD, USA). The numbers of NKA-IR cells and HA-IR cells in the lamellae and interlamellar regions were standardized as the number of NKA-IR cells and HA-IR cells per mm length of the lamellae or interlamellar region.

2.9. Immunofluorescence detection of NKA-, VHA-, NHE- and NKCC-immunoreactive cells

For double staining of different antibodies, the whole-mount immunofluorescence detection was used. Gills were fixed with 4% paraformaldehyde in PBS (pH 7.4) for 1–2 h at 4 °C. After a 2 min wash with PBS three times, gills were postfixed and permeabilized with 70% ethanol at −20 °C for 20 min. After a 2 min wash with PBS three

times, samples were incubated with 5% BSA for 30 min to block nonspecific binding. Samples were then incubated overnight at 4 °C with a polyclonal antibody against the VHA and NHE (polyclonal antibody; diluted 1:500, respectively). After washing with PBS three times for 10 min, gills were further incubated in goat-anti-mouse IgG Alexa fluor 546 (diluted 1:400, Molecular Probes) for 2 h at RT and washed with PBS three times for 10 min. For double staining of NKA and NKCC (diluted 1:400 and 1:200, respectively), gills were then incubated for 2 h at RT. After washing with PBS three times for 10 min, gills were further incubated in goat-anti-rabbit IgG Alexa fluor 488 (diluted 1:400, Molecular Probes) for 1 h at RT and washed with PBS three times for 10 min. Observations and image acquisitions were made using a Zeiss confocal laser scanning microscope (LSM 510; Germany). The image software was Zeiss LSM image browser.

2.10. Experimental protocol

The effects of DW and 10 g/L over 4 days on *T. microlepis* were examined using the following parameters: (1) cumulative mortality on the fourth day of the experiments, plasma osmolality and Na^+ concentration, MWC and stress proteins (hsp70 and hsp90) in each experimental period; (2) protein expression and enzyme-specific activity of NKA and VHA; (3) immunohistochemical detection of NKA-IR cells and HA-IR cells in the lamellar and interlamellar regions; and (4) immunofluorescence detection of NKA-, VHA-, NHE- and NKCC. The FW group was considered the control group. Fish were transferred to 15 g/L and physiological responses, including plasma osmolality, MWC, and stress protein expression, were measured at approximately 6 h. Beyond this period, most fish had died and further observation was not possible.

2.11. Statistical analysis

All values are presented as mean ± SEM. For statistical analyses, results were analyzed using one-way ANOVA and Dunnett's test by comparing them with the control group (FW group). Differences were considered statistically significant where $p<0.05$. All statistical analyses were conducted using SAS 9.1 for Windows (SAS Institute, Cary, NC, USA).

3. Results

3.1. Plasma analysis and muscle water content

The plasma osmolalities of *T. microlepis* ranged from 270–325 mOsm/kg when the fish was acclimated in DW and 10 g/L treatments. The plasma osmolality and MWC were not significantly different in fish that received the DW and FW treatment (Fig. 1). However, the plasma osmolality increased accordingly to the environmental salinity (one-way ANOVA, $F_{3,25}=64.3$, $p<0.001$). The MWC value was maintained in the 10 g/L treatment but decreased in the 15 g/L treatment (one-way ANOVA, $F_{3,32}=12.02$, $p<0.01$). Plasma Na^+ concentration was higher in salinity treatments (one-way ANOVA, $F_{3,27}=23.88$, $p<0.01$, DW treatment: 89.33 ± 4.03 mM; FW treatment: 88.59 ± 8.17 mM; 10 g/L treatment: 144.44 ± 5.88 mM; 15 g/L treatment: 126.09 ± 9.35 mM). Mortality increased with increasing salinity and was three times as high in the 10 g/L treatment compared to the FW treatment. No fish survived in the 15 g/L treatment for more than 6 h (Table 1).

3.2. Immunoblotting analysis protein abundance

An increase in heat shock proteins is a response to environmental stress (Smith et al., 1999; Palmisano et al., 2000; Pan et al., 2000). Immunoblots of total gill lysates of the DW, FW, 10 g/L, and 15 g/L treatments all revealed single immunoreactive bands of hsp70 and hsp90, respectively (Fig. 2A). Further comparisons of the protein abundance of hsp70 and hsp90 revealed a higher relative abundance with increasing salinity (hsp70, one-way ANOVA, $F_{3,31}=14.00$, $p<0.001$; hsp90, one-way ANOVA, $F_{3,31}=3.42$, $p=0.0308$) (Fig. 2C and D).

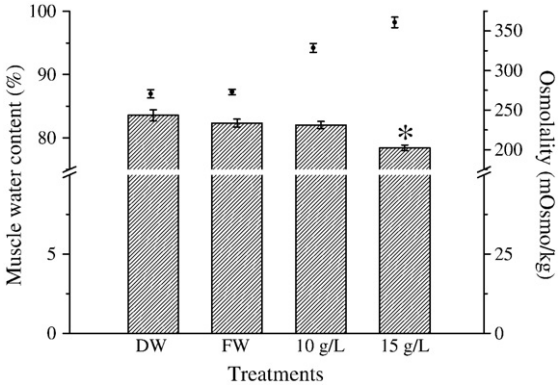

Fig. 1. Plasma osmolality (mOsm/kg) ($N=5$–8, in closed circles) and muscle water content ($N=10$, in histograms) of *T. microlepis* in the DW, FW, 10 g/L, and 15 g/L treatments. The plasma osmolality and MWC of DW did not differ significantly from those of the control group (FW). The plasma osmolality increased with environmental salinity ($p<0.001$), but the MWC was maintained in the 10 g/L treatment and decreased in the 15 g/L treatment ($p<0.01$). Values are represented as mean ± SEM. The asterisk indicates a significant difference compared to the control group (Dunnett's test).

Immunoblots of total gill lysates of the DW, FW, and 10 g/L treatments all revealed single immunoreactive bands of NKA at approximately 95 kDa molecular mass. The VHA had two immunoreactive bands at approximately 70 kDa molecular mass (Fig. 2B). Based on image analysis, the highest relative abundance of the NKA α-subunit was found in the 10 g/L treatment (one-way ANOVA, $F_{2,22}=19.55$, $p<0.01$), while the DW treatment showed no difference compared with the FW treatment (Fig. 3A). The highest relative abundance of the VHA was also found in the 10 g/L treatment (one-way ANOVA, $F_{2,22}=3.77$, $p=0.04$), while the DW treatment was not different from FW (Fig. 3B).

3.3. NKA and VHA enzyme activity

The specific activity of NKA in *T. microlepis* was significantly higher in the DW and 10 g/L treatments than in the control treatment; it was approximately 1.4- and 2.5-fold of the FW treatment, respectively (one-way ANOVA, $F_{2,24}=18.92$, $p<0.01$) (Fig. 3C). The specific activity of VHA in *T. microlepis* was significantly higher in the DW treatment, i.e., approximately 2.0-fold of the FW treatment (one-way ANOVA, $F_{2,28}=4.28$, $p=0.0239$). No difference was observed in the 10 g/L treatment compared to FW (Fig. 3D). Our experiments aimed to test the extent to which low Na^+ would affect VHA in *T. microlepis*. However, different pH conditions prevailed between the DW and control groups, i.e., 7.14 ± 0.08 and 7.81 ± 0.10, respectively (Table 1). Therefore, we could not conclude whether the increased VHA activity was a result of low Na^+ or acid secretion or both. Hence, we designed another experiment with a pH of 7.20 (osmolality: 3 mOsm/kg; Na^+ concentration: 1.26 mM, commercial mineral water, Uni-President, Taiwan) and a control group with a pH of 7.80 (osmolality: 3 mOsm/kg; Na^+ concentration: 1.24 mM) and determined the VHA activity between these two groups. The osmolality and Na^+ concentration showed no differences between these two groups. Thus, different pH values between 7.20 and 7.80 did not affect VHA activity in *T. microlepis* (VHA activity in pH 7.20 was 0.43 ± 0.03; in pH 7.80 it was 0.44 ± 0.08, $p=0.869$, $N=7$). Therefore, the higher VHA activity in DW resulted from low Na^+ but not from pH conditions.

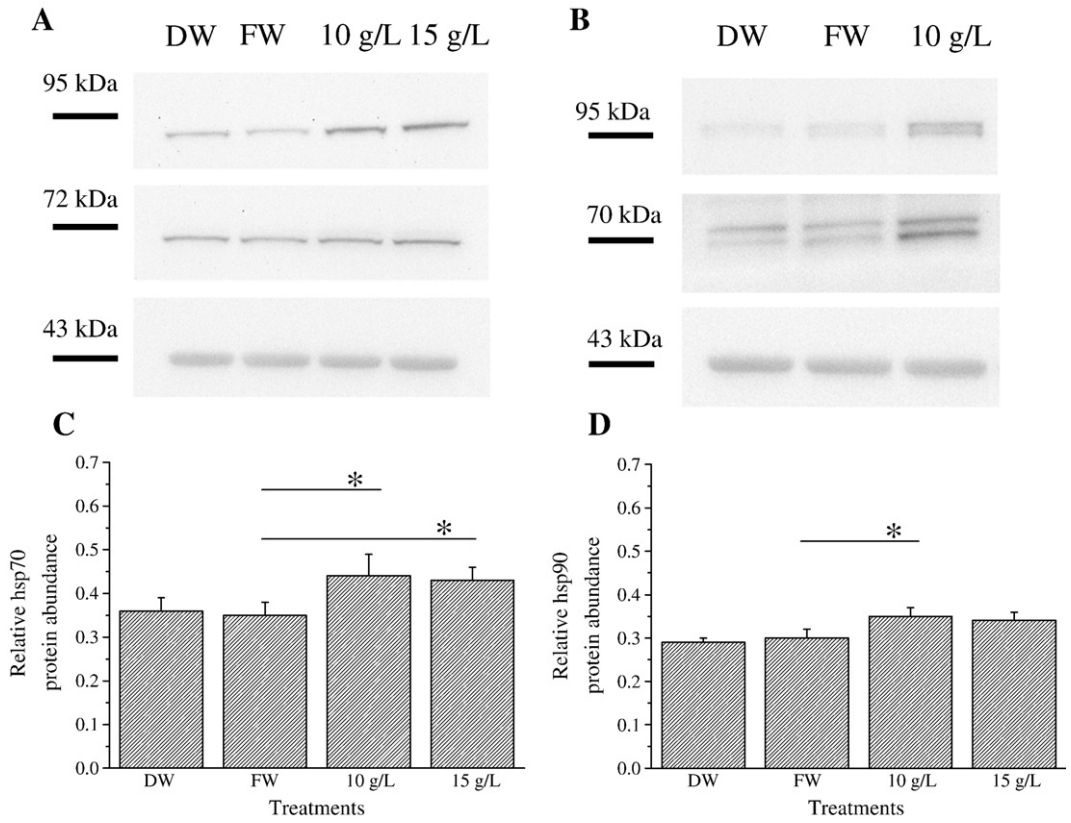

Fig. 2. Protein expression in gills of *T. microlepis* in DW, FW, 10 g/L, and 15 g/L treatments. (A) Immunoblots of total gill lysates of the DW, FW, 10 g/L, and 15 g/L treatments all revealed single immunoreactive bands of hsp70 and hsp90, respectively. Comparisons of the protein abundance of hsp70 and hsp90 revealed a higher relative abundance with increasing salinity ($N=8$). (B) Immunoblots of total gill lysates of the DW, FW, and 10 g/L treatments all revealed single immunoreactive bands of NKA at approximately 95 kDa molecular mass. The VHA proteins showed two immunoreactive bands of approximately 70 molecular mass. The β-actin showed single immunoreactive bands at 43 kDa molecular mass. (C) (D) Intensities of immunoreactive bands of hsp70 and hsp90 proteins in gills of *T. microlepis* of different salinity groups revealed those showed the highest relative abundance salinity treatment ($p<0.05$).

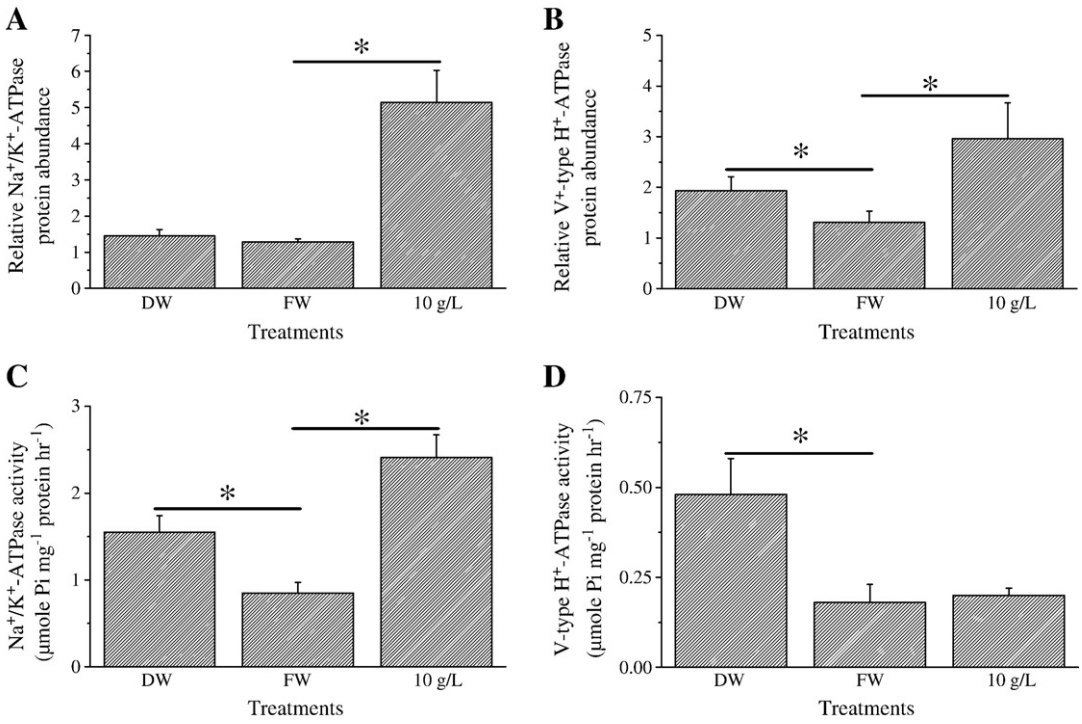

Fig. 3. Intensities of immunoreactive bands of protein in gills of *T. microlepis* of different salinity groups revealed: (A) the highest relative abundance of the NKA α-subunit was found in the 10 g/L treatment ($p<0.01$); no difference was observed between the DW and FW treatments; (B) VHA immunoreactivity was higher in the DW and 10 g/L treatments than in FW ($p<0.05$). Gill NKA and VHA activities of *T. microlepis* were in the DW, FW, and 10 g/L treatments; (C) the specific activity of NKA was significantly higher in the DW and 10 g/L treatments than in FW (approximately 1.4- and 2.5-fold, respectively; $p<0.01$); and (D) the specific activity of VHA was significantly higher only in the DW treatment (approximately 2.0-fold; $p<0.05$). Values are presented as mean ± SEM ($N=8$). The asterisk indicates a significant difference compared to the control group (Dunnett's test).

3.4. Immunohistochemical detection of NKA- and VHA-immunoreactive cells

The gill NKA-IR cells and HA-IR cells of the control group were distributed both in the lamellar and interlamellar region. *T. microlepis* gills had three different cell populations as follows: (1) NKA-IR cells (black arrowhead); (2) both NKA-IR- and HA-IR cells (white arrowhead); and (3) HA-IR cells (arrow) (Fig. 4A, B). Interestingly, a greater NKA-IR population was found in the gill than other cell types (Fig. 4C).

The NKA-IR cells of the DW (Fig. 5A), FW (Fig. 5B), and 10 g/L (Fig. 5C) treatments were distributed in the lamellar and interlamellar regions. The HA-IR cells of the DW (Fig. 5E), FW (Fig. 5F), and 10 g/L (Fig. 5G) treatments were also distributed in the lamellar and interlamellar regions. There was a significant increase in the number of NKA-IR cells in the lamellar (one-way ANOVA, $F_{2,21}=14.43$, $p<0.001$) (Fig. 5I) and interlamellar (one-way ANOVA, $F_{2,21}=7.72$, $p<0.05$) (Fig. 5J) regions in the DW and 10 g/L treatments compared to that in the FW treatment. Moreover, there was a significant increase in the number of HA-IR cells in the lamellar region in the DW and 10 g/L treatments compared to that in the FW treatment (one-way ANOVA, $F_{2,21}=11.70$, $p<0.001$)(Fig. 5K). However, in the interlamellar region, there was no difference in the number of HA-IR cells among the three treatments (Fig. 5L).

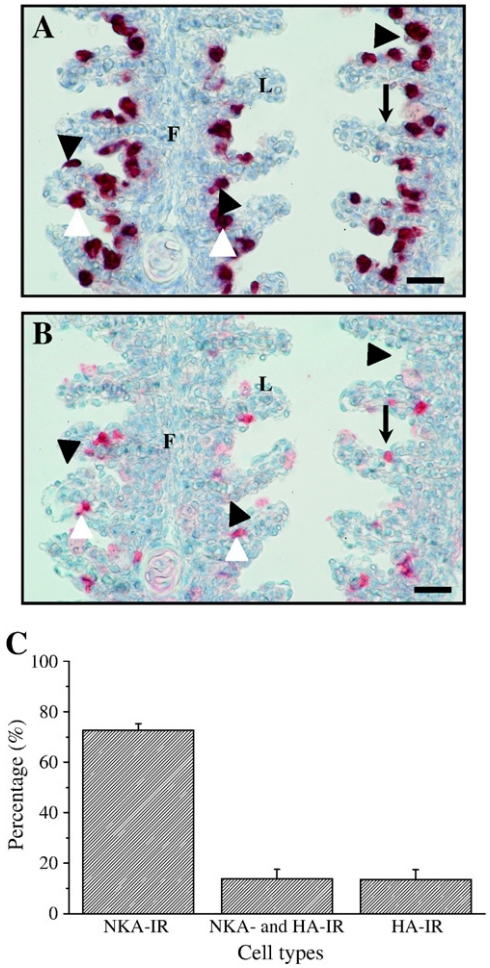

Fig. 4. Immunohistochemical detection of NKA- and VHA-immunoreactive cells of *T. microlepis*. The gill NKA-IR cells (A) and HA-IR cells (B) from the FW treatment were distributed in both the lamellar and interlamellar regions. *Trichogaster microlepis* showed three different cell populations in the gills: (1) NKA-IR cells (black arrowhead); (2) both NKA-IR and HA-IR cells (white arrowhead); and (3) HA-IR cells (arrow). Interestingly, (C) the cells of the NKA-IR population were found more frequently than were other cell types in the gill lamellae. F, filament; L, lamellar. Scale bar, 30 μm ($N=8$).

3.5. Immunofluorescence detection of NKA-, VHA-, NHE- and NKCC-immunoreactive cells

Whole-mount immunofluorescence images were used to define the subtypes of ionocytes in the gills of *T. microlepis*. We found that NKA (green) and VHA (red) were not co-localized in the same cell (Fig. 6A). Similarly, NKA (green) and NHE (red) (Fig. 6B), and NKCC (green) and VHA (red) were also not co-localized (Fig. 6C). Immunofluorescence staining indicated that NKCC was distributed in the apical region (Fig. 6D). Some cells like in Fig. 6B contain both NHE and NKA, and may not be co-staining because a whole-mount method was used to detect the immunofluorescence reaction, making a different observation to cells next to it.

4. Discussion

All anabantoid species with a labyrinth organ are continuous air-breathing fish in normoxic and hypoxic environments. In our previous study, the NKA activity of the first and secondary gills of *T. leeri* were up-regulated significantly in the deionized water (Huang et al., 2008), and this genus was also found in the estuary. There is less information about the ionoregulatory ability in the gill of the aquatic air-breathing fish. Therefore, this study aimed to determine whether gill NKA and VHA differ in their expression in an aquatic air-breathing fish, *T. microlepis* across a range of salinities.

4.1. Physiological responses of fishes for different salinity tolerances

T. microlepis is distributed in fresh water and sometimes in estuarine environments. The plasma osmolality of *T. microlepis* increased in 10 g/L and 15 g/L treatments. The increased plasma osmolality with salinity has been described in tilapia (*Oreochromis mossambicus*) and medaka (*Oryzias latipes*) (Lee et al., 2000; Kang et al., 2008). Moreover, the mortality and plasma Na^+ concentration were considerably higher in the 15 g/L treatment than in the 10 g/L treatment. The MWC of *T. microlepis* was maintained at approximately 80–85% among the DW, FW, and 10 g/L treatments but decreased to 75% in the 15 g/L treatment. MWC is an indicator for the osmoregulatory capacity in euryhaline teleosts (Woo and Chung, 1995; Kelly et al., 1999b), and the decreasing MWC in *T. microlepis* indicated that the fish underwent osmotic stress and loss of osmoregulatory functions in the 15 g/L treatment. The 15 g/L treatment (427 mOsm/kg) resulted in extreme osmolality stress due to the fact that the osmoregulatory mechanisms of *T. microlepis* (360 mOsm/kg) could not function efficiently; fish would die within 6 h and no individual survived up to 12 h in this treatment. The higher hsp90 and hsp70 levels at these salinities were an indication that 10–15 g/L is a critical upper salinity tolerance. From some literature the heat shock proteins presented the environmental stress in load on the teleost, such as salinity and temperature (Smith et al., 1999; Palmisano et al., 2000; Pan et al., 2000). Therefore, the expressions of the shock proteins showed both the salinity and stress responses for the fish gill.

4.2. NKA and VHA protein abundance and activity

Changes in gill NKA activity in response to salinity changes or environmental disturbances were found in many teleosts (Kelly and Woo, 1999; Marshall et al., 2002; Perry et al., 2003; Hwang and Lee, 2007; Huang et al., 2008). The increased expression in both NKA and VHA in the 10 g/L treatment was an indication that *T. microlepis* are active osmoregulators in this hyperosmotic environment. NKA activity increased in the 10 g/L treatment, and NKA and VHA activities increased in the DW treatment. The lower ion concentration resulted in an up-regulation of NKA activity to enhance ion uptake across gills (Perry, 1997; Evans et al., 2005). From the 10 g/L treatment potential shifts in plasma pH, it is possible that the increase in NKA activity at this salinity is to facilitate acid–base regulation. The expression among

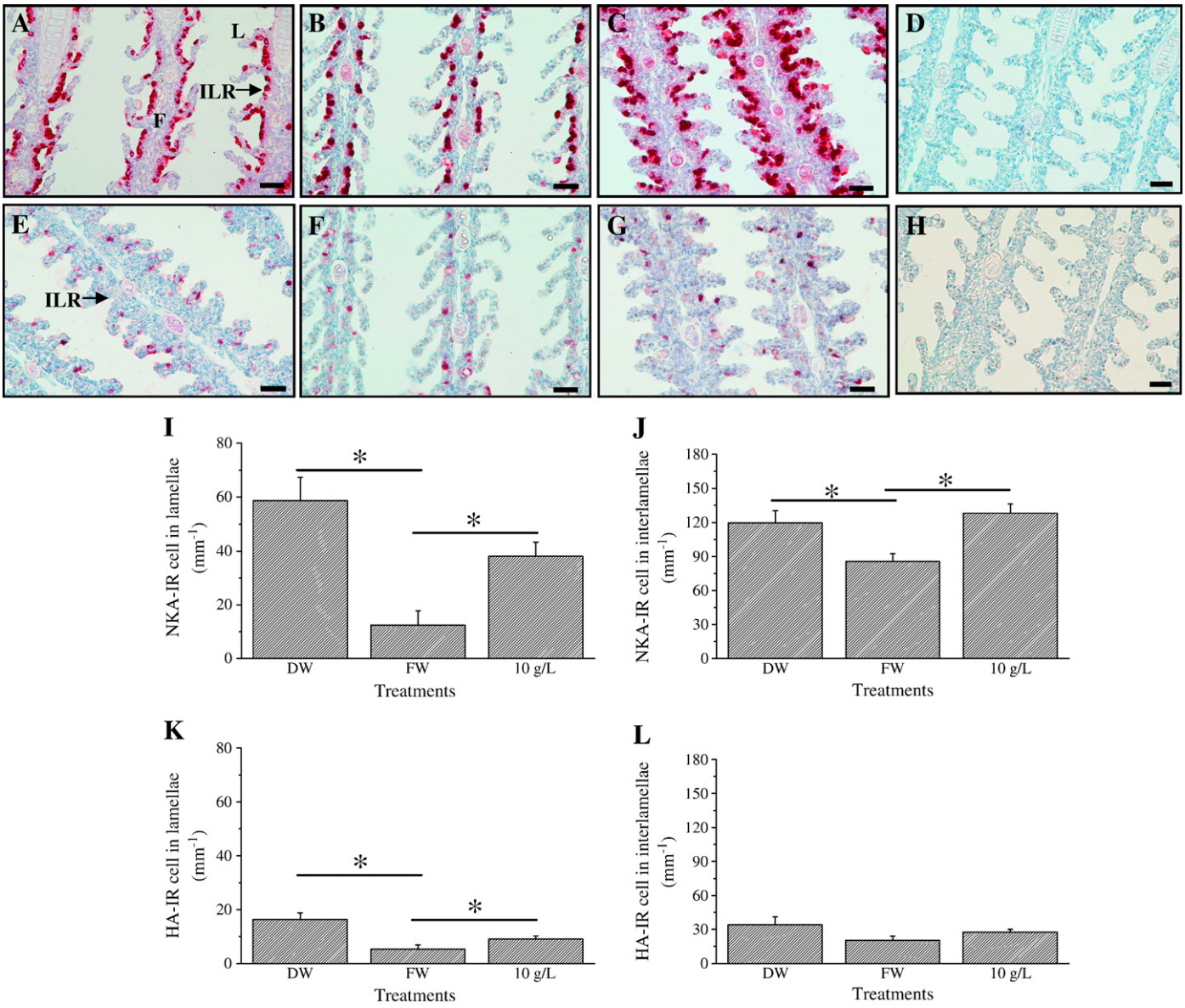

Fig. 5. Immunohistochemical detection of NKA- and VHA-immunoreactive cells of *T. microlepis*. The gill NKA-IR cells in the DW (A), FW (B), and 10 g/L treatment (C) groups were distributed in the gill lamellar and interlamellar regions. The gill HA-IR cells in the DW (E), FW (F), and 10 g/L treatment (G) groups were also distributed in the gill lamellar and interlamellar regions. We included negative controls in the NKA and VHA staining (D, H). F, filament; L, lamellar; ILR, interlamellar region. The amounts of NKA-IR and HA-IR cells were determined from the lamellar and interlamellar regions of *T. microlepis* in the DW, FW, and 10 g/L treatments. (I) The amounts of NKA-IR cells in the lamellar region in the DW and 10 g/L treatments were greater than those in the FW one ($p<0.001$). (J) Similarly, significantly more NKA-IR cells were observed in the interlamellar region in the DW and 10 g/L treatments compared to FW ($p<0.05$). (K) The amounts of HA-IR cells in the gill lamellar region were significantly higher in the DW treatment ($p<0.001$) compared to those in the FW and 10 g/L treatments. (L) There was no difference in the number of HA-IR cells among the three groups in the interlamellar region. Values are presented as mean ± SEM ($N=8$). Scale bar, 30 μm. The asterisk indicates a significant difference compared to the control group (Dunnett's test).

osmoregulatory proteins will help to explain the salinity tolerance of *T. microlepis*. The physiological response of NKA and VHA activity in the present study was consistent with the hypothesis that enzyme activity is lowest in primary natural habitats (Hwang and Lee, 2007).

In the past, using pharmacological, physiological, immunocytochemical, and molecular approaches, VHA was known to play a role in apical Na^+ uptake in the epithelial cells of fish gills (Beyenbach and Wieczork, 2006; Horng et al., 2007; Hwang and Lee, 2007). The VHA heterologous antibody used in the present study recognized two major bands in *T. microlepis*, both at approximately 70 kDa, as the predicted sizes. It is possible that two VHA A-subunits exist with different but close molecular weights in *T. microlepis*. A similar finding was reported in rainbow trout, *Oncorhynchus mykiss*, by Katoh et al. (2006). VHA plays a role in Na^+ uptake and H^+ secretion in the skin and possibly the gills of zebrafish (Horng et al., 2007). Besides, VHA not only participates in ion/osmoregulation but also has a role in acid–base balance (Perry et al., 2003; Tresguerres et al., 2005, 2007a,b).

4.3. NKA- and VHA-immunoreactive cells

Mitochondria-rich cells, the major ionocytes in fish gills, have been well documented in earlier studies (Perry et al., 2003; Hirose et al., 2003; Hwang and Lee, 2007). According to the model of ionic regulatory mechanisms for zebrafish gill/skin ionocytes, three different subtypes of ionocytes were identified, including NaR cells (NKA-rich), HR cells (VHA-rich and NKA-few), and NCC cells (Hwang and Lee, 2007; Hwang,

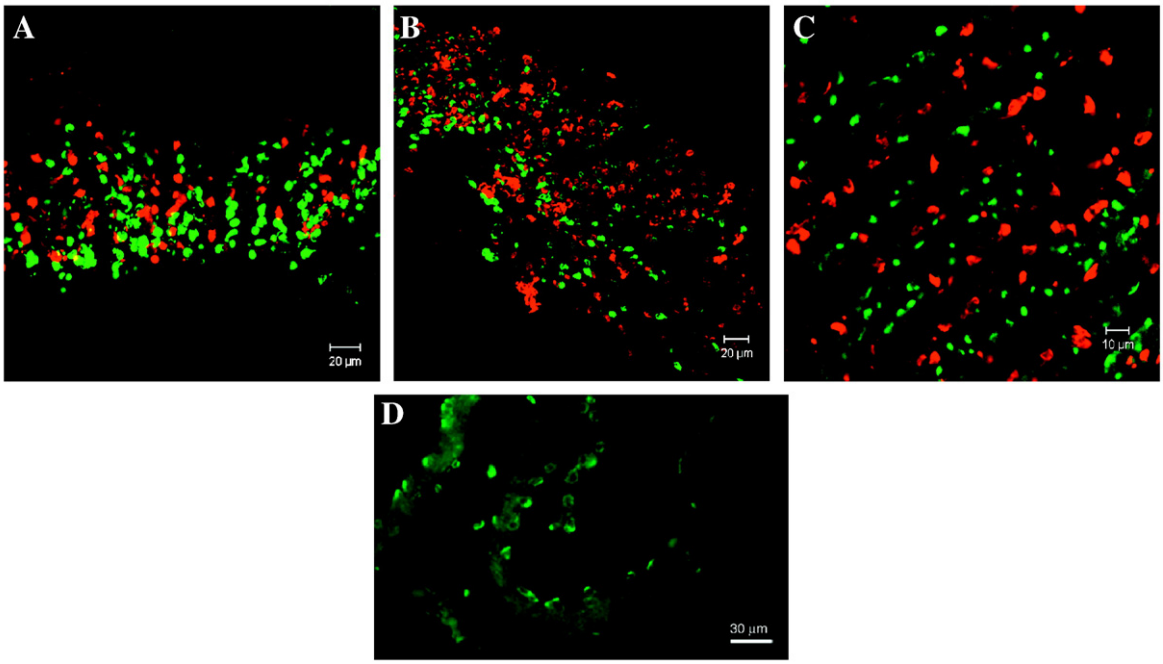

Fig. 6. Confocal whole-mount immunofluorescence images of the gill in *T. microlepis*. (A) Double staining of NKA (green) and VHA (red). (B) Double staining of NKA (green) and NHE (red). (C) Double staining of NKCC (green) and VHA (red). (D) Apical distribution of NKCC in the immunofluorescence staining. (For interpretation of the references to color in this figure legend, the reader is referred to the web version of this article.)

2009). In the present study, we found at least three different cell populations: (1) NKA-IR cells (equivalent to NaR cells); (2) both NKA-IR and HA-IR cells (equivalent to HR cells); and (3) HA-IR cells. Further, NKA-IR cells in the lamellae of *T. microlepis* gills ou t-numbered the other two cell types (both NKA-IR and HA-IR cells and HA-IR cells), and correspondingly, they might play a greater role in osmoregulatory function. In addition to the similar pattern in the immunoreactive expressions of the NaR cells and HR cells to the patterns observed in zebrafish gills, *T. microlepis* had another cell type in which only HA-IR cells can be stained. From the study of other teleosts, there are many ionocyte types in the gills, and our observation may be a species-specific expression. In the dogfish (*Squalus acanthias*), using an immunocytochemical method, NKA and VHA were not found in the same cells but NHE2 was found in both types of cells (Claiborne et al., 2008).

The number of NKA-IR cells in the lamellar and interlamellar regions in the gill increased following exposure to DW and 10 g/L treatments for 4 days compared to FW, and the number of HA-IR cells only increased in the lamellar region after being transferred to the DW treatment. The increase in the number of MRCs has been documented in the air-breathing fish, *Hypostomus CF. plecostomus* and *Hypostomus tiensis* (Fernandes and Perna-Martins, 2001, 2002) in DW. The gill lamellar region is the major gas-exchange site, and when a fish can exchange gases from other parts of the body, such as accessory air-breathing organs, the gill lamellae would play a role in alternative physiological functions such as osmoregulation (Lin and Sung, 2003).

Since it would take 4 days to increase in the cell number (Huang et al., 2008), the increases in the activities of two major ion transporters, NKA and VHA, were more likely a combination from the increases in the molecular activity on transporters and the protein abundance.

4.4. Immunofluorescence detection of NKA-, VHA-, NHE- and NKCC-immunoreactive cells

According to previous studies, there are at least two models concerning apical transport of Na^+ in fish gill cells, including: (1) an apical VHA electrically linked with ENaC; and (2) an electroneutral exchange of an apical NHE (Hirose et al., 2003; Hwang and Lee, 2007). Recent studies have elucidated the role of NHE in Na^+ transport in fish gills (Choe et al., 2005; Esaki et al., 2007; Yan et al., 2007). The model for Cl^- uptake is supported by an important candidate ion-transporter, NKCC/NCC. The antibody used to detect both NKCC1a and NCC was a mouse monoclonal antibody against 310 amino acids at the C-terminus of human colonic NKCC1, and has been used in many teleosts (Scott et al., 2004; Gamba, 2005; Hiroi and McCormick, 2007; Inokuchi et al., 2008). Na^+/Cl^- cotransporter (NCC) belongs to a member of the cation-chloride cotransporter family, which includes the NKCC1 and NKCC2 families, and is supposed to have an apical distribution with an ion-absorptive function similar to NKA-positive MRCs in FW killifish (Hwang and Lee, 2007; Katoh et al., 2008). The results of the immunofluorescence detection, the apical NKCC in the epithelial cells of *T. microlepis* might be correlated to its ionic uptake functions (Katoh et al., 2008). Some studies indicated that the NKCC is on the basolateral side of MRCs in the gills of killifish, and its role in actively absorbing Cl^- across the gills in freshwater is still unclear (Patrick and Wood, 1999). Therefore, the pathways in Cl^- uptake need more investigation. We found that the NHE was not co-localized with NKA in the lamellae and the NKA also was not co-localized with VHA. In addition, the NKCC protein was not co-localized with VHA and in the apical region of the epithelium cell. Thus, the subtypes of ionocytes in *T. microlepis* may be similar to the zebrafish model (Hwang and Lee, 2007; Hwang, 2009). The different results between the immunohistochemical detection and immunofluorescence detection may result from the methodological limitations. The locations of the gill by whole-mount and different fluorescence intensity may lose some information in the immunofluorescence detection. Therefore, there might have been some discrepant results between two methods. Another mechanism was also found in zebrafish larvae recently in which Cl^- uptake is dependent on Cl^-/HCO_3^- exchangers under normal conditions (Bayaa et al., 2009). Whether this protein also plays the same role in *T. microlepis* is another issue.

In conclusion, the NKA and VHA response was evaluated in *T. microlepis* for different salinity tolerances. The mortality, plasma

osmolalities, and plasma Na^+ concentration was higher in the 10 g/L treatment, and MWC decreased in the 15 g/L treatment. The highest NKA and VHA protein abundances were found in the gills of the 10 g/L treatment. The NKA and VHA activity was the highest in the DW treatment; the NKA activity in the 10 g/L treatment was equally high. *T. microlepis* was identified to possess at least three ionocytes by immunohistochemical detection, including NKA-IR cells, both NKA-IR and HA-IR cells, and HA-IR cells. The number of NKA-IR cells in the gill lamellae and interlamellar regions significantly increased in the DW and 10 g/L treatments; however, only the number of HA-IR cells in the gill lamellae region increased in the DW treatment. The proposed model of ion regulatory mechanisms of gill ionocytes and NKCC-IR (similar to NCC cells in zebrafish) in aquatic air-breathing fish needs to be investigated further for clarity. *T. microlepis* exhibited an osmoregulatory ability in DW and 10 g/L treatments, and the branchial NKA and VHA responses were different for different salinity tolerances. Our study has provided further insights into the mechanisms of osmoregulation in the aquatic air-breathing fish, *T. microlepis*.

Acknowledgements

Grant sponsor: National Science Council (NSC 93-2311-B-029-006 and NSC 94-2621-B-029-002) to HCL.

References

Bayaa, M., Vulesevic, B., Esbaugh, A., Braun, M., Eller, M.E., Grosell, M., Perry, S.F., 2009. The involvement of SLC26 anion transporters in chloride uptake in zebrafish (*Danio rerio*) larvae. J. Exp. Biol. 212, 3283–3295.

Beyenbach, K.W., Wieczork, H., 2006. The V-type H^+-ATPase: molecular structure and function, physiological roles and regulation. J. Exp. Biol. 209, 577–589.

Burggren, W.W., 1979. Bimodal gas exchange during variation in environmental oxygen and carbon dioxide in *Trichogaster trichopterus*. J. Exp. Biol. 82, 197–213.

Choe, K.P., Kato, A., Hirose, S., Plata, C., Sindic, A., Romero, M.F., Claiborné, J.B., Evans, D. H., 2005. NHE3 in an ancestral vertebrate: primary sequence, distribution, localization, and function in gills. Am. J. Physiol. Regul. Integr. Comp. Physiol. 289, R1520–R1534.

Claiborne, J.B., Choe, K.P., Morrison-Shetkar, A.I., Weakley, J.C., Havird, J., Freiji, A., Evans, D.H., Edwards, S.L., 2008. Molecular detection and immunological localization of gill Na^+/H^+ exchanger in the dogfish (*Squalus acathias*). Am. J. Physiol. Regul. Integr. Comp. Physiol. 294, R1092–R1102.

Esaki, M., Hoshijima, K., Kobayashi, S., Fukuda, H., Kawakami, K., Hirose, S., 2007. Visualization in zebrafish larvae of Na^+ uptake in mitochondria-rich cells whose differentiation is dependent on foxi3a. Am. J. Physiol. Regul. Integr. Comp. Physiol. 292, R470–R480.

Evans, D.H., 1999. Ionic transport in the fish gill epithelium. J. Exp. Zool. 283, 641–652.

Evans, D.H., Piermarini, P.M., Choe, K.P., 2005. The multifunctional fish gill: dominant site of gas exchange, osmoregulation, acid–base regulation, and excretion of nitrogenous waste. Physiol. Rev. 85, 97–177.

Fernandes, M.N., Perna-Martins, S.A., 2001. Epithelial gill cells in the armored catfish, *Hypostomus CF. plecostomus* (Loricaridae). Rev. Bras. Biol. 61, 69–78.

Fernandes, M.N., Perna-Martins, S.A., 2002. Chloride cell responses to long-term exposure to distilled and hard water in the gill of the armored catfish, *Hypostomus tietensis* (Loricariidae). Acta Zool. 83, 321–328.

Gamba, G., 2005. Molecular physiology and pathophysiology of electroneutral cationchloride cotransporters. Physiol. Rev. 85, 423–493.

Graham, J.B., 1997. Air-breathing fishes: evolution, diversity, and adaptation. Academic Press, New York.

Hiroi, J., McCormick, S.D., 2007. Variation in salinity tolerance, gill Na^+/K^+-ATPase, $Na^+/K^+/2Cl^-$ cotransporter and mitochondria-rich cell distribution in three salmonids *Salvelinus namaycush*, *Salvelinus fontinalis* and *Salmo salar*. J. Exp. Biol. 210, 1015–1024.

Hiroi, J., Yasumasu, S., McCirmick, S.D., Hwang, P.P., Kaneko, T., 2008. Evidence for an apical Na-Cl cotransporter involved in ion uptake in a teleost fish. J. Exp. Biol. 211, 2584–2599.

Hirose, S., Kaneko, T., Naito, N., Takei, Y., 2003. Molecular biology of major components of chloride cells. Comp. Biochem. Physiol. B 136, 593–620.

Horng, J.L., Lin, L.Y., Huang, C.J., Katoh, F., Kaneko, T., Hwang, P.P., 2007. Knockdown of V-ATPase subunit A (atp6v1a) impairs acid secretion and ion balance in zebrafish (*Danio rerio*). Am. J. Physiol. Regul. Integr. Comp. Physiol. 292, R2068–R2076.

Huang, C.Y., Lee, W., Lin, H.C., 2008. Functional differentiation in the anterior gills of the aquatic air-breathing fish, *Trichogaster leeri*. J. Comp. Physiol. B 178, 111–121.

Hwang, P.P., 2009. Ion uptake and acid secretion in zebrafish (*Danio rerio*). J. Exp. Biol. 212, 1745–1752.

Hwang, P.P., Lee, T.H., 2007. New insights into fish ion regulation and mitochondrion-rich cells. Comp. Biochem. Physiol. 148, 479–497.

Imsland, A.K., Gunnarsson, S., Foss, A., Stefansson, S.O., 2003. Gill Na^+-K^+-ATPase activity, plasma chloride and osmolality in juvenile turbot (*Scophthalmus maximus*) reared at different temperatures and salinities. Aquaculture 218, 671–683.

Inokuchi, M., Hiroi, J., Watanabe, S., Lee, K.M., Kaneko, T., 2008. Gene expression and morphological localization of NHE3, NCC and NKCC1a in branchial mitochondria-rich cells of Mozambique tilapia (*Oreochromis mossambicus*) acclimated to a wide range of salinities. Comp. Biochem. Physiol. 151, 151–158.

Kang, C.K., Tsai, S.C., Lee, T.H., Hwang, P.P., 2008. Differential expression of branchial Na^+/K^+-ATPase of two medaka species, *Oryzias latipes* and *Oryzias dancena*, with different salinity tolerances acclimated to fresh water, brackish water and seawater. Comp. Biochem. Physiol. 151, 566–575.

Katoh, F., Hyodo, S., Kaneko, T., 2003. Vacuolar-type proton pump in the basolateral plasma membrane energizes ion uptake in branchial mitochondria-rich cells of killifish *Fundulus heteroclitus*, adapted to a low ion environment. J. Exp. Biol. 206, 793–803.

Katoh, F., Tresguerres, M., Lee, K.M., Kaneko, T., Aida, K., Goss, G.G., 2006. Cloning of rainbow trout SLC26A1: involvement in renal sulfate secretion. Am. J. Physiol. Regul. Integr. Comp. Physiol. 290, R1468–R1478.

Katoh, F., Cozzi, R.R.F., Marshall, W.S., Goss, G.G., 2008. Distinct $Na^+/K^+/2Cl^-$ cotransporter localization in kidneys and gills of two euryhaline species, rainbow trout and killifish. Cell Tissue Res. 334, 265–281.

Kelly, S.P., Woo, N.Y.S., 1999. The response of sea bream following abrupt hyposmotic exposure. J. Fish Biol. 55, 732–750.

Kelly, S.P., Chow, I.N.K., Woo, N.Y.S., 1999a. Alteration in Na^+–K^+-ATPase activity and gill chloride cell morphometrics of juvenile black sea bream (*Mylio macrocephalus*) in response to salinity and ration size. Aquaculture 172, 351–367.

Kelly, S.P., Chow, I.N.K., Woo, N.Y.S., 1999b. Halopalasticity of black seabream (*Mylio macrocephalus*): hypersaline to freshwater acclimation. J. Exp. Zool. 283, 226–241.

Lee, T.H., Hwang, P.P., Shieh, Y.E., Lin, C.H., 2000. The relationship between 'deep-hole' mitochondria-rich cells and salinity adaptation in the euryhaline teleost, *Oreochromis mossambicus*. Fish Physiol. Biochem. 23, 133–140.

Lin, H.C., Sung, W.T., 2003. The distribution of mitochondria-rich cells in the gills of air-breathing fish. Physiol. Biochem. Zool. 76, 215–222.

Lin, Y.M., Chen, C.N., Lee, T.H., 2003. The expression of gill Na, K-ATPase in milkfish, *Chanos chanos*, acclimated to seawater, brackish water and fresh water. Comp. Biochem. Physiol. 135, 489–497.

Lin, C.H., Tsai, R.S., Lee, T.H., 2004. Expression and distribution of Na^+, K^+-ATPase in gills and kidneys of the green spotted pufferfish, *Tetraodon nigroviridis*, in response to salinity challenge. Comp. Biochem. Physiol. 138, 287–295.

Lin, Y.M., Chen, C.N., Yoshinaga, T., Tsai, S.C., Shen, I.D., Lee, T.H., 2006. Short-term effects of hyposmotic shock on Na^+/K^+-ATPase expression in gills of the euryhaline milkfish, *Chanos chanos*. Comp. Biochem. Physiol. A 143, 406–415.

Marshall, W.S., Lynch, E.M., Cozzi, R.R., 2002. Redistribution of immunofluorescence of CFTR anion channel and NKCC cotransporter in chloride cells during adaptation of the killifish *Fundulus heteroclitus* to sea water. J. Exp. Biol. 205, 1265–1273.

Morgan, J.D., Iwama, G.K., 1998. Salinity effects on oxygen consumption, gill Na^+, K^+-ATPase and ion regulation in juvenile Coho salmon. J. Fish Biol. 53, 1110–1119.

Moron, S.E., Fernandes, M.N., 1996. Pavement cell ultrastructural differences on *Hoplias malabaicus* gill epithelia. J. Fish Biol. 49, 357–362.

Munshi, J.S.D., Olson, K.R., Ojha, J., Ghosh, T.K., 1986. Morphology and vascular anatomy of the accessory respiratory organs of the air-breathing climbing perch, *Anabas testudineus* (Bloch). Am. J. Anat. 176, 321–331.

Olson, K.R., 2002. Vascular anatomy of the fish gill. J. Exp. Zool. 293, 214–231.

Olson, K.R., Munshi, J.S.D., Ghosh, T.K., Ojha, J., 1986. Gill microcirculation of the air-breathing climbing perch, *Anabas testudineus* (Bloch): relationships with the accessory respiratory organs and systemic circulation. Am. J. Anat. 176, 305–320.

Olson, K.R., Roy, P.K., Ghosh, T.K., Munshi, J.S.D., 1994. Microcirculation of gills and accessory respiratory organs from the air-breathing snakehead fish, *Channa punctata*, *C. gachua*, and *C. marulius*. Anat. Rec. 238, 92–107.

Olson, K.R., Ghosh, T.K., Roy, P.K., Munshi, J.S.D., 1995. Microcirculation of gills and accessory respiratory organs of the walking catfish *Clarias batrachus*. Anat. Rec. 242, 383–399.

Palmisano, A.N., Winton, J.R., Dickhoff, W.W., 2000. Tissue-specific induction of Hsp90 mRNA and plasma cortisol response in Chinook salmon following heat shock, seawater challenge, and handling challenge. Mar. Biotechnol. 2, 329–338.

Pan, F.P., Zarate, J.M., Tremblay, G.C., Bradley, T.M., 2000. Cloning and characterization of Salmon hsp90 cDNA: upregulation by thermal and hyperosmotic stress. J. Exp. Zool. 287, 199–212.

Patrick, M.L., Wood, C.M., 1999. Ion and acid–base regulation in freshwater mummichog (*Fundulus heteroclitus*): a departure from the standard model for freshwater teleosts. Comp. Biochem. Physiol. A 122, 445–456.

Perry, S.F., 1997. The chloride cell: structure and function in the gills of freshwater fishes. Annu. Rev. Physiol. 59, 325–347.

Perry, S.F., 1998. Relationships between branchial chloride cells and gas transfer in freshwater fish. J. Exp. Biol. 119, 9–16.

Perry, S.F., Shahsavarani, A., Georgalis, T., Bayaa, M., Furimsky, M., Thomas, S.L., 2003. Channels, pumps, and exchangers in the gill and kidney of freshwater fishes: their role in ionic and acid–base regulation. J. Exp. Zool. 300, 53–62.

Peterson, G.L., 1978. A simplified method for analysis of inorganic phosphate in the presence of interfering substances. Anal. Biochem. 84, 164–172.

Scott, G.R., Richards, J.G., Forbush, B., Isenring, P., Schulte, P.M., 2004. Changes in gene expression in gills of the euryhaline killifish *Fundulus heteroclitus* after abrupt salinity transfer. Am. J. Physiol. Cell Physiol. 287, C300–C309.

Smith, T.D., Tremblay, G.C., Bradley, T.M., 1999. Hsp70 and a 54 kDa protein (Osp54) are induced in salmon (*Salmo salar*) in response to hyperosmotic stress. J. Exp. Zool. 284, 286–298.

Tresguerres, M., Katoh, F., Fenton, H., Jasinska, E., Goss, G.G., 2005. Regulation of branchial V-H^+-ATPase, Na^+/K^+-ATPase and NHE2 in response to acid and base infusion in the Pacific spiny dogfish (*Squalus acanthias*). J. Exp. Biol. 208, 345–354.

Tresguerres, M., Parks, S.K., Goss, G.G., 2007a. Recovery from blood alkalosis in the Pacific hagfish (*Eptatretus stoutii*): Involvement of gill V-H^+-ATPase and Na^+/K^+-ATPase. Comp. Biochem. Physiol. 148, 133–141.

Tresguerres, M., Parks, S.K., Wood, C.M., Goss, G.G., 2007b. V-H^+-ATPase translocation during blood alkalosis in dogfish gills: interaction with carbonic anhydrase and involvement in the postfeeding alkaline tide. Am. J. Physiol. Regul. Integr. Comp. Physiol. 292, R2012–R2019.

Watanabe, S., Nida, M., Maruyama, T., Kaneko, T., 2008. Na^+/H^+ exchanger isoform 3 expressed in apical membrane of gill mitochondrion-rich cells in Mozambique tilapia *Oreochromis mossambicus*. Fish. Sci. 74, 813–821.

Woo, N.Y.S., Chung, K.C., 1995. Tolerance of *Pomacanthus imperator* to hypoosmotic salinities: changes in body composition and hepatic enzyme activities. J. Fish Biol. 47, 70–81.

Yan, J.J., Chou, M.Y., Kaneko, T., Hwang, P.P., 2007. Gene expression of Na^+/H^+ exchanger in zebrafish H^+-ATPase-rich cells during acclimation to low-Na^+ and acidic environments. Am. J. Physiol. Cell Physiol. 293, C1814–C1823.